

Component Damage From Printed Circuit Board Loading

D. H. Duffner, R. W. Klopp, A. Wagner-Jauregg, R. A. Sire, and E. M. Webster
Exponent Failure Analysis Associates
Menlo Park, CA

Abstract

Electronic components are being used in increasingly more severe shock environments. This combined with an industry trend of increased component reliability to help reduce electronic system downtime has created an increasing demand for understanding the loads imparted through a printed circuit board (PCB) to an individual component on the board. Local stiffening of the circuit board can limit the component loads, however stiffening devices can be costly to design and implement. They are also bulky, taking up valuable space on already crowded PCBs. Both experimentation and analytical tools were used here to investigate how loads are transmitted through a circuit board to an individual component.

Two case histories are presented that investigate how specific loads applied to a circuit board may damage individual components. In the first case history, failures of surface mounted capacitors were occurring at some point during the PCB assembly process. In order to isolate the specific step in the assembly process that was causing the damage, miniature strain gages were adhered in several locations adjacent to the subject capacitors. The strains were monitored as the instrumented PCB was put through its normal assembly process. The measured strains at the gage locations were compared to the reported strength of the capacitors.

In the second case history, a PCB carrying a single ceramic column grid array (CCGA) package was subjected to static and shock loading. Strain gages were adhered to the CCGA and the PCB near the CCGA to measure the level and duration of static and shock strains imparted during typical PCB handling, and insertion into, and removal from, a multiple board chassis. The highest magnitude shock loads resulted from PCB bending, and occurred as the printed circuit board connector contacted its mate on the chassis.

A finite element analysis of the circuit board and CCGA was conducted to infer from strains measured near the CCGA the individual solder column loads that might result from the PCB insertion and removal. It is these pins that sometimes fail during use. It is suspected that high pin loads from PCB shock loads significantly lower the lifetime of a CCGA. CCGA pin loads are determined from the finite element analysis for a given PCB load, and compared to the ultimate tensile strength of the subject material.

Introduction

Will my printed circuit board, along with its many attached components, survive the loads to which it will be subjected over the course of its lifetime, or will it suffer a perhaps premature and unexpected failure? This question is rarely explicitly asked, however a portion of the design process is typically dedicated to ensuring the correct answer. Two case histories will be discussed where some common measurement and analytical techniques are used to compare component stresses to strengths.

In the first case, the goal is to determine if the component stresses that arise from a known PCB manufacturing process are the culprit in causing capacitor failures. In the second case, the effort was focused on pin loads in a CCGA.

Case History 1 – Capacitor Cracking

Surface mounted capacitors mounted on PCBs were suffering failures even before being put into service. Loads applied to the PCB during manufacture were suspected of bending the board, and straining the subject capacitors beyond the manufacturers

allowable limit. One particular test conducted during the manufacturing process was suspected of producing these high strain levels.

Strain gages were adhered to the PCBs, and the strain levels monitored while the board went through its normal manufacturing steps, including the subject test. The testing involved placing the board into a chamber; a mechanism clamps the board in place while probes are held firmly against several contact points. It was believed that the out-of-plane forces applied to the board as the probes came into contact bend the board to a level such that the allowable strains to the capacitors were exceeded.

Strain Gage Testing

Strain measurements were performed at two locations on the surface of each of two different circuit boards as the boards were cycled through a loading sequence in the subject test chamber. The subject boards were numbered 60016 (Figure 1) and 60021 (Figure 2).



Figure 1 – PCB 60016 with Capacitors 168 and 169



Figure 2 – PCB 60021 with Capacitors 5 and 111

Micro-Measurements brand EA -13-031CE-350 strain gages were bonded adjacent to capacitors C168 and C169, on board 60016; and adjacent to capacitors C5 and C111, on board 60021. Figure 3 shows a typical installed strain gage, in this case adjacent to C168 on board 60016. The gages were bonded using Micro-Measurements M-Bond 200 adhesive, and oriented so that the strain measurement was parallel to a line running from solder terminal to solder terminal on the capacitors, that is, parallel to the short direction of the boards.

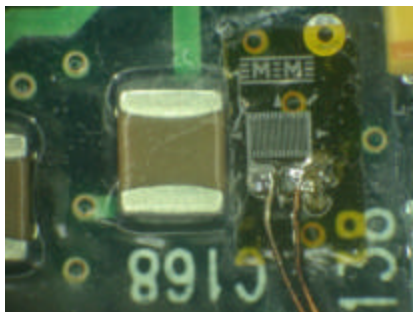


Figure 3 – Closeup View Near Capacitor 168 Showing Strain Gage Location

The gages were wired in a quarter-bridge configuration to Micro-Measurements Model 2310 bridge completion amplifiers. The amplifiers were in turn connected to a laptop computer-based data acquisition system. Tests were performed by starting the data acquisition system, cycling the test machine “on,” pausing a few seconds, then cycling the machine “off.” The total acquisition window was 12 seconds. The tests shown were repeated 3 times.

The recorded voltages were converted to strains and the signal filtered to reduce noise. Strain histories at each of the four capacitor locations are shown in Figure 4 for one set of three “on-off” cycles of the tester. The central portion of each history corresponds to the tester being in the “on” position.

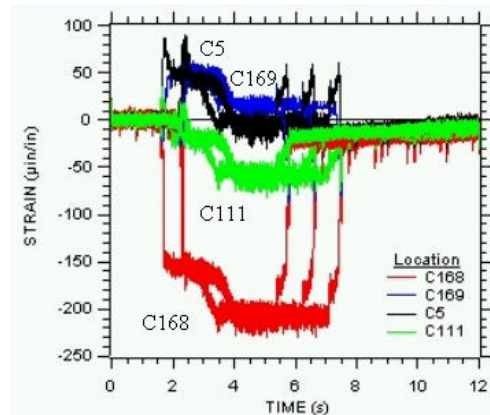


Figure 4 – Strain Histories for the First Set of 3 “On-Off” Tester Cycles

A second set of results is presented in Figure 5. Between the first and second sets, the lid of the tester was opened and closed. There appears to be significant variation in strain histories associated with capacitors C169, C5, and C111, following opening and closing of the lid of the test machine. Note in particular that the sign of the strain when the tester is “on” is reversed for capacitors C169 and C5 between Figures 4 and 5. Apparently, opening and closing the tester can result in significant changes in the mechanical boundary conditions acting on the board.

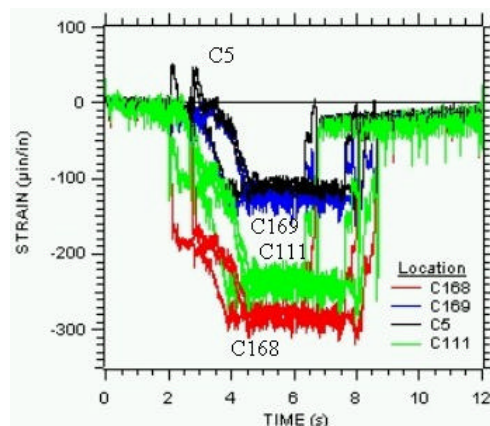


Figure 5 – Strain Histories for the Second Set of 3 “On-Off” Tester Cycles

From comparison of the figures, we see that the largest strain magnitude is about 300 microinches per inch ($\mu\text{in/in}$) compressive measured adjacent to C168 as seen in Figure 5. The highest measured tensile strain was 90 $\mu\text{in/in}$ measured adjacent to capacitor C5 as seen in Figure 4.

Case 1 Results

Failure of these ceramic capacitors reportedly occurs when the strain is in the 1300 to 2500 $\mu\text{in}/\text{in}$ tension range¹. The highest measured tensile strain of 90 $\mu\text{in}/\text{in}$ is far below this value. Thus the tester in question was not the culprit behind the capacitor failures.

Even though the measured strain is far less than the reported failure strain, it is important to recognize two things: first, the measured strain is not directly comparable to this failure strain, because the board is being bent, not pulled in tension. The strain through the thickness of the capacitor varies, and depends upon where the neutral axis of the capacitor/board combination lies. Further analysis is required to determine the precise strain distribution². Second, failures can be time dependent. Many repetitions of strain (fatigue) amplitudes of much smaller than the ultimate strain can also result in failure.

Case History 2 – CCGA Pin Loads

Concern had arisen that PCB bending normally expected in service, might damage the solder columns on a CCGA package. Specifically, bending loads from chassis interconnection were thought to produce damaging axial loads in the pins.

The subject CCGA has 1247 columns made of a 90% lead, 10% tin alloy. Figure 6 shows a typical CCGA, circuit board, and chassis. Also shown are two of the four strain gages used for testing, and their associated wiring.



Figure 6 – CCGA, Circuit Board and Chassis

Our goal was to know the solder column loads due to PCB bending. Since direct measurement of the loads was impractical due to small size and inaccessibility, we combined a hybrid experimental and analytical approach to solve the problem. We used strain gage measurements to find the strains near the CCGA due to bending loads applied remotely. We then performed finite element analysis to relate the strains near the CCGA to solder column loads

Three identical circuit boards, identified as A, B, and C, were used for the testing. Circuit board C had no components installed and was tested to measure its

stiffness (Young's Modulus) for input into the finite element model. Circuit board A was configured for measurement of chassis insertion loads; this board included a chassis slot mating connector. Circuit board B had no connector and was used to measure PCB bending sensitivity. The board deflection and strain gage output were monitored while a force was applied to the tip of the board. The connector was left off of board B to facilitate clamping to the bench top.

Strain Gage Installation

Strain gage tests were conducted on circuit boards A, and B. Four strain gages were adhered in identical locations to each of the two circuit boards. The PCB dimensions are 15.6 inches (in.) long by 5 in. wide, and .125 in. thick. The CCGA dimensions are 1.67 in. long by 1.28 in. wide, and its center is located 4.7 in. from the connector end of the board, and 2.4 in. from the top edge of the board.

Strain gage 1 was located on the backside of the circuit board, 1.2 in. toward the top from the center of the CCGA. Gage 2 was also located on the backside of the circuit board, directly at the center of the CCGA. Gage locations 1 and 2 are shown in Figure 7. Gage 3 was located on the front, or CCGA, side of the circuit board directly above gage number 1, 1.2 in. toward the top from the center of the CCGA. Gage 4 was located directly in the center of the CCGA lid. Gage locations 3 and 4 can be seen in Figure 8. All four gages were wired in a $\frac{1}{4}$ bridge configuration.

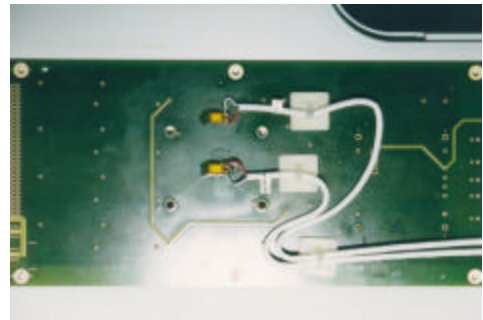


Figure 7 – Backside of Circuit Board Showing Strain Gage Locations 1 and 2

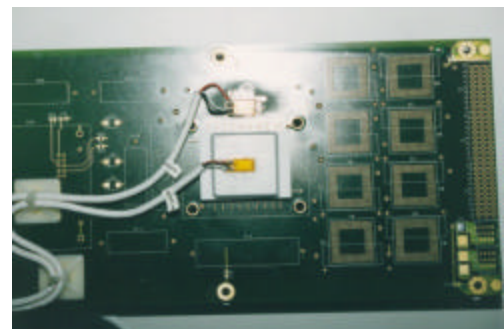


Figure 8 – Front of Circuit Board Showing Strain Gage Locations 3 and 4

These locations were selected to provide an overall board bending strain remote from the CCGA, in addition to the local strains of the CCGA lid and circuit board below the CCGA. Bending strain is of primary importance, since the highest tensile loads in the columns result from circuit board bending. The suspected highest bending strains occur along the length of the board. It is assumed that no twisting, bending along the width, or thickness of the board occurred during the tests.

The strain gage readings on the front and back of the circuit board were combined to read in bending strain and axial strain instead of their raw outputs. Because of the nature of their installation, the board bending strain is gage number 3 (top) strain MINUS gage number 1 (bottom) strain divided by two. In this sense, a positive bending strain will make the board curve away from the CCGA, or “frown”, and a negative bending strain will make it curve towards it, or “smile”. The board tension strain is gage number 3 strain PLUS gage number 1 strain divided by two.

Bending Sensitivity

Circuit board B was clamped at its connector end to a lab bench top. All four channels of strain data, and circuit board tip deflection were recorded as incremental loads were added to the tip of the circuit board. The point of load application measured 14.19 in. from the edge of the clamp and 10.25 in. from the center of the CCGA.

The load was increased in 0.5 to 1 pound (lbf) increments up to a maximum load of nearly 3.5 lbf. The board was unloaded, and the test repeated once more. The results of the testing are shown in Table 1, along with an adjustment made for the 0.7 in. strain gage offset from the center of the area modeled with finite elements. The values shown are the slopes of the linear-least-squares fit to the load versus strain data. The PCB bending sensitivity was 129 $\mu\text{in/in/lb}$ of tip load.

Table 1 – Results of Bending Sensitivity Test; Tabulated Values are for Board Tip Load Applied 10.25 Inches from the Center of CCGA

	Board Bending Near CCGA	Circuit Board Bottom Below CCGA	CCGA Lid Center
Strain Per Unit Tip Load (min/in/lbf)	129	-54	27
Bending Moment Per Unit Strain at Gage 1-3 Location (in-lf/min/in)	0.079	-1.190	0.380
Bending Moment Per Unit Strain at Gage 1-3 Location (in-lf/min/in)	0.074	-0.177	0.354

Insertion and Removal Strains

Circuit board A was used for insertion and removal tests into and out of the chassis. The strains from the four gages were recorded at high speed with a PC based digital data acquisition system. The system was set to record 2500 samples per strain gage per second. Each test lasted three seconds.

The test method consisted of a rapid insertion by hand for three inches into the chassis slot. The rapid insertion continued until the insertion lever engaged the chassis. At this point, the insertion lever was raised by hand until the board reached full insertion, and the connector was fully engaged. Both insertion steps were captured in the single three-second-test window. Four insertion tests were conducted in slots 6 and 7 (two each). After each insertion test, a removal test was conducted. The insertion / removal test configuration is shown in Figure 6.

Figure 9 shows the bending and axial strain results from a typical insertion test (test 25, slot number 6). The second high amplitude axial strain pulse shown to the right in Figure 10 is the slower, lever insertion portion of the test. In this test the peak bending strain first reached +60 $\mu\text{in/in}$, then -60 $\mu\text{in/in}$. The peak axial strain reached -40 $\mu\text{in/in}$. Note that the peak maximum and minimum bending strains are reached prior to the highest amplitude axial strain (connector engagement), and occur at a relatively higher frequency. Figure 10 shows the strains measured at locations 2 and 4 during the same insertion test as shown in Figure 9.

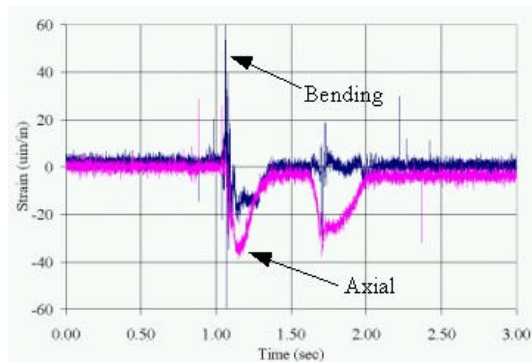


Figure 9 – Circuit Board Bending and Axial Strains Recorded from gage Locations 1 and 3 for Insertion Test Number 25 into Slot 6

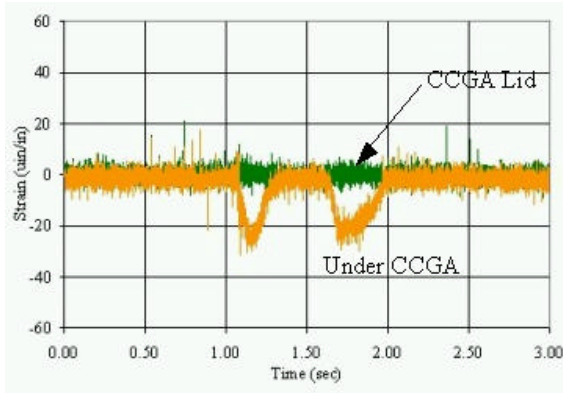


Figure 10 – Board Strain Gage 2 Under CCGA and CCGA Lid Strain Gage 4 for Insertion Test Number 25 into Slot 6

Figure 11 shows the bending and axial strain gage results for a typical card removal. This is the card removal immediately following the insertion discussed above (test number 26, slot 6). Note that, consistent with the insertion test, the maximum bending strain does not occur until after the primary connector disengagement, and that it occurs at a relatively high frequency. The summary of the insertion test results is given in Table 2. The summary includes only the maximum and minimum bending strains, since this is the condition of highest column axial load.

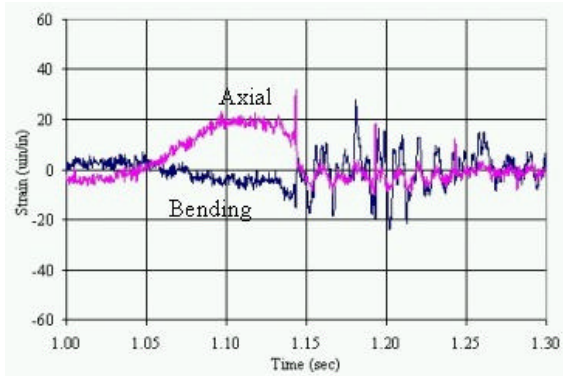


Figure 11 – Circuit Board Bending and Axial Strains Recorded from Gage Locations 1 and 3 for Removal Test Number 26 from Slot 6

Table 2 – Maximum and Minimum Bending Strains at Gage Locations 1 and 3, Measured During the Insertion Tests

Test Number	Insertion Slot	Maximum Bending (min/in)	Minimum Bending (min/in)
25	6	60	-60
27	6	51	-47
29	7	45	-39
31	7	56	-58

Finite Element Analysis

A linear, elastic, computer based finite element analysis (FEA) was conducted with ANSYS software. A localized finite element model was created using the dimensions shown in Figure 12. These dimensions were measured from a sample dummy CCGA (no die included) sectioned into fourths. The column dimensions are not shown in Figure 12, but are as follows: diameter = 0.02 in., length = 0.087 in., and pitch = .039 / in.

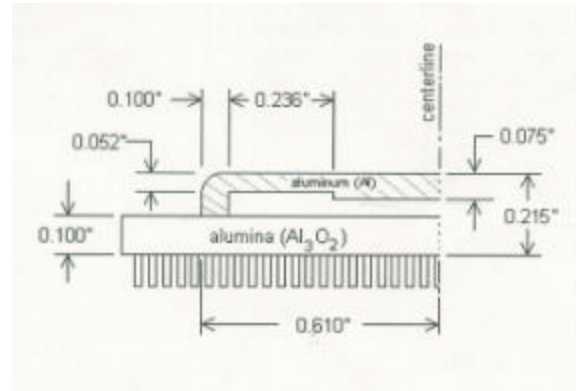


Figure 12 – Cross Section View of CCGA These Measurements were used as Inputs to the FEA

The mechanical properties for the various components are given in Table 3. Because the mechanical properties of the circuit board were not readily available, and can vary significantly with board design, mechanical tests were conducted to determine the tensile modulus of elasticity, or Young's modulus. Two specimens were cut from board C. Figure 13 shows the results for specimen 1. The elastic modulus is the slope of the curve, and measures 3.17 million pounds per square inch (psi) for specimen 1, and 3.10 million psi for specimen 2. The average of these two values is given in Table 3, and used in the FEA.

Table 3 – Mechanical Properties of the Various Components that Make Up the CCGA and Circuit Board

Component	Material	Young's Modulus (x10 ⁶ psi)	Poisson's Ratio
PC Board	Glass, Copper, Polymer	3.14	0.30
Columns ^{6,7}	90% Lead, 10% Tin, solder	2.76	0.40
Base ^{3,4}	Ceramic (Alumina)	50.0	0.23
Chip ⁵	Silicon	27.0	0.28
Lid	Aluminum	10.6	0.33

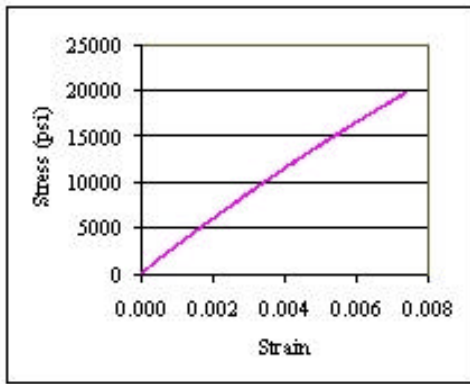


Figure 13 – Stress vs. Strain Output Plot for Mechanical Test of Circuit Board Specimen 1

Since the CCGA and circuit board are symmetric about two orthogonal centerline cross sections (quarter symmetry), only one fourth of the CCGA and surrounding circuit board were modeled. As seen in Figure 4, enough of the surrounding circuit board was modeled to include the locations of strain gages adhered to the circuit board surface for the load testing. The FEA model is square, and extends down and to the left 1.4 in. from the center of CCGA as seen in Figure 14. This area includes the strain gage adhered 1.2 in. down from the center of the CCGA. Another strain gage is located on the backside of the circuit board directly below the gage shown in Figure 14. A third strain gage was located directly in the center of the CCGA lid, and a fourth located directly below on the backside of the circuit board.

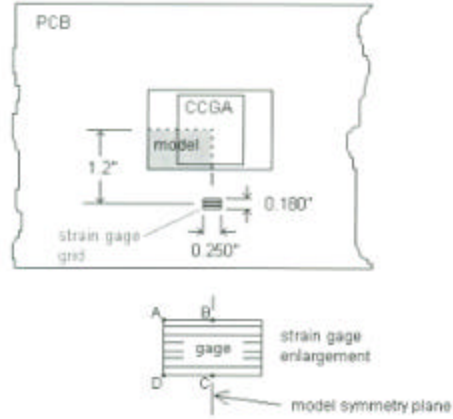


Figure 14 – Quarter Symmetry Model Showing CCGA, Circuit Board, and One Strain Gage Location

Figure 15 shows the finite element model used in our analysis. One quarter of the CCGA module can be seen here, along with a local portion of the circuit board. The edge of the model shown to the right was rotated to produce a uniform bending moment along the length of the board. The left edge of the board was held fixed in the length and width direction to allow for symmetry along the centerline cross sections.

Figure 16 shows two overlaid cross sections of the model. Deflections have been scaled up by a factor of 20 here to make them more visible. In this analysis we forced the circuit board to bend toward the CCGA. Since the model is linear however, the same results can be used for the case when the board is bent in the opposite direction as well.

Figure 17 shows the predicted column loads for the -10 inch-pound (in-lbf) applied bending moment. The maximum amplitude column load is -1.736 lbf, and occurs in the two outboard columns along the short edge of the CCGA (8 columns on the full CCGA). For the load case shown in Figure 16, this load is compressive. The maximum tensile load for this load case is 0.503 lbf and occurs in several columns along the long edge of the CCGA.

For the opposite load case, when the board bends in the opposite direction, the maximum amplitude load of 1.736 lbf is tensile, and the maximum amplitude compressive load is -0.503 lbf. As seen in Figure 17, the load amplitude drops off rapidly on the columns immediately inboard of the edge rows.

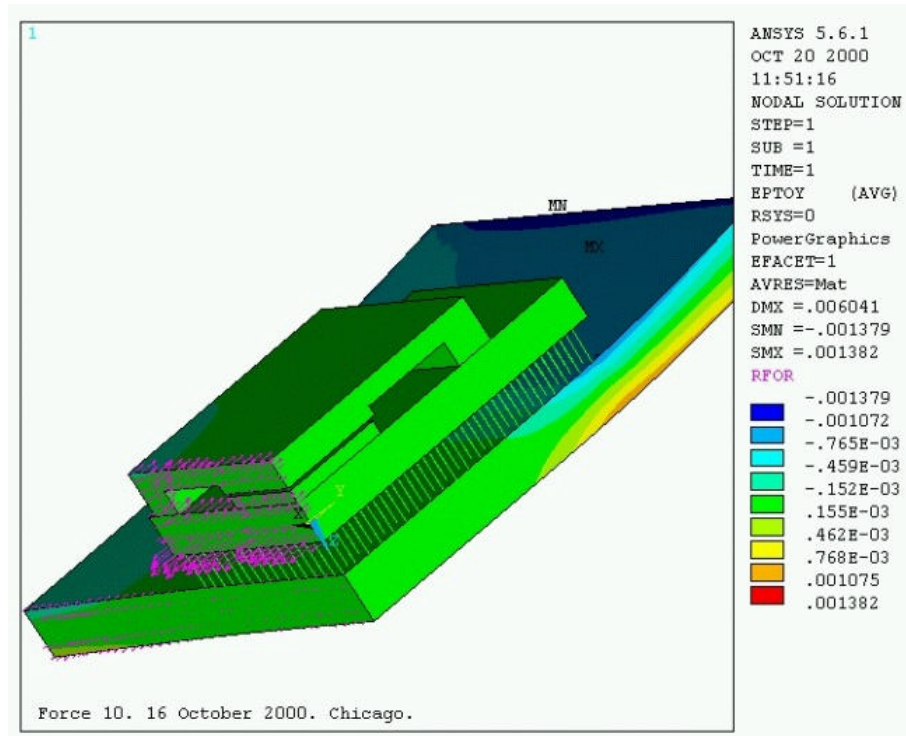


Figure 15 – Finite Element Model Shown Under Load

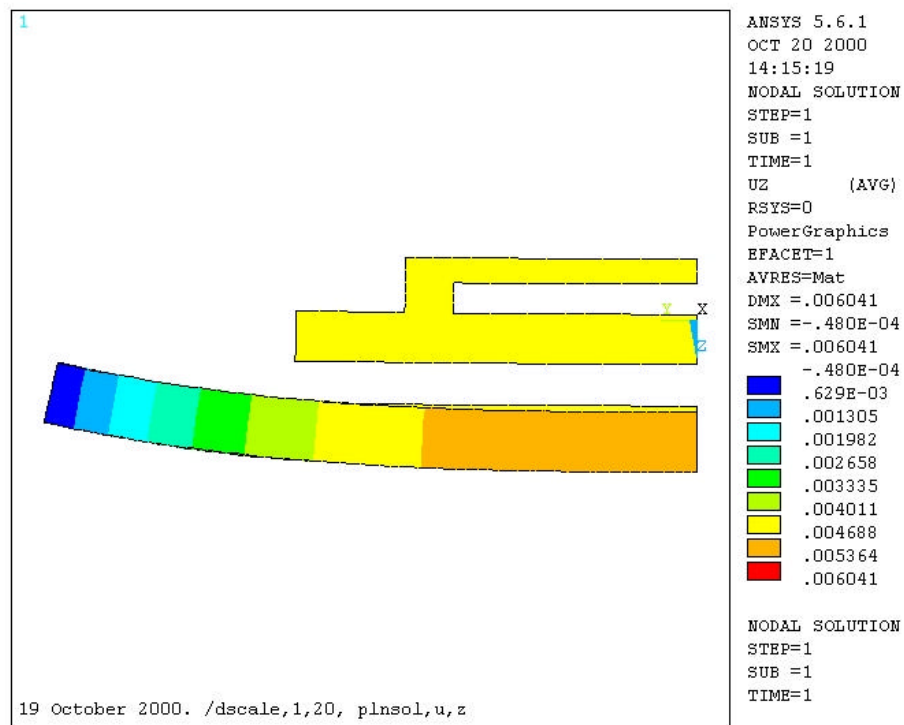


Figure 16 – Overlaid Cross Section of the Model Deflections Scaled Up by a Factor of 20 Portion of Circuit Board Away from CCGA is More Flexible

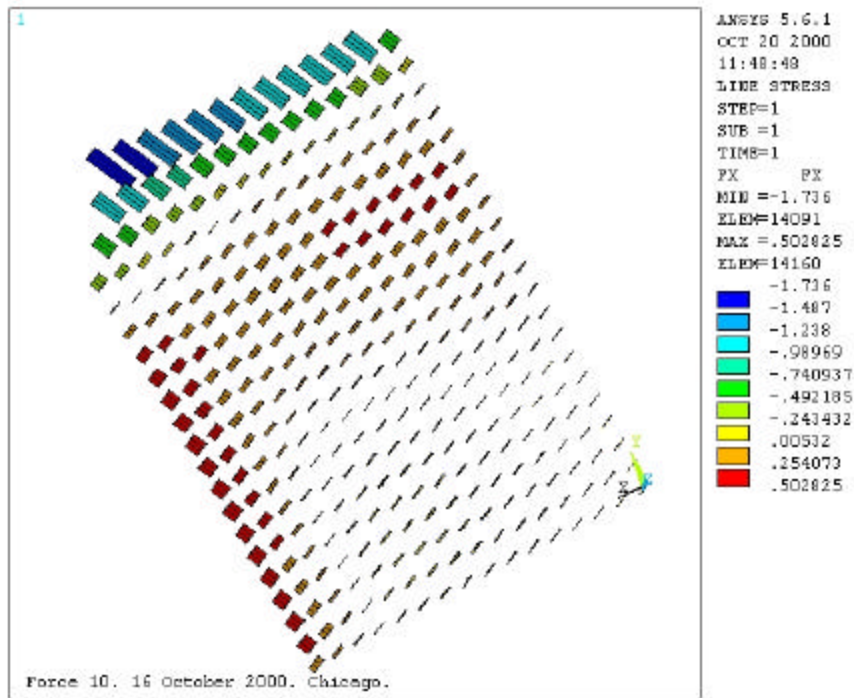


Figure 17 – ANSYS Results Plot Showing the Column Loads Predicted by the FEA for a –10 in-lbf Moment the Maximum Amplitude Load is –1.736 lbf

Case 2 Results

The finite element analysis results are shown in Table 4. These results predicts that for a 10 in-lbf moment applied to the circuit board the maximum column force is 1.736 lbf, and occurs at just eight columns, two in each of the four corners. Combining the inferred sensitivity of column load to bending moment in Table 4 with the measured sensitivity of bending moment to strain in Table 1, yields the sensitivity of column load to measured strain shown in Table 5.

The highest measured insertion test bending strain was 60 $\mu\text{in/in}$. Applying the sensitivity in Table 5 results in a load at the eight most highly loaded columns of 0.78 lbf. The ultimate strength of the column material, 90% lead, 10% tin, is 4400 psi. Given the specified column diameter of 0.020 in, the column ultimate load is 1.38 lbf. The strain gage testing, and FEA predict that the insertion test load is equivalent to 57% of the material's tensile ultimate strength for the eight most highly loaded columns. While this load will not fail the column in a single cycle, repeated application over several thousand cycles may result in fatigue failures.

Conclusions

The two case histories presented here have shown that predictions of circuit board reliability can be made using a combination of strain gage testing and analytical tools such as finite element analysis. In the first case of surface mounted capacitors, the

measured strain on the surface of the circuit board adjacent to the component of interest was measured and provides an example of a means to assess the component reliability based on allowable strains. As seen in the second case of the CCGA, more complex geometries and load paths require the use of analytical tools such as finite element analysis in addition to strain gage testing to predict circuit board reliability.

References

1. Jim Bergenthal, "Ceramic Chip Capacitors 'Flex Cracks,' Understanding and Solutions," KEMET Electronics Corporation, 1998.
2. Dave S. Steinberg, Vibration Analysis for Electronic Equipment, John Wiley & Sons, 1988.
3. IBM ASIC SA-12E Packaging Databook, International Business Machines, June 2000.
4. C. A. Harper, Electronic Packaging and Interconnection Handbook, Third Edition, McGraw-Hill, 2000.
5. P. Gwozdz, "Semiconductor Processing Technology for Field Service Engineers," Semiconductor Equipment and Materials International, Version 4.1, May 1994.
6. Metals Handbook, Volume 6, Welding Brazing, and Soldering, Ninth Edition, American Society for Metals, 1983.
7. Mark's Standard Handbook for Mechanical Engineers, Eight Edition, T. Baumeister Editor, McGraw-Hill, 1978.